

Measuring Forces in Liver Cutting for Reality-Based Haptic Display¹

Teeranoot Chanthasopeephan, Jaydev P. Desai², Alan C. W. Lau

Program for Robotics, Intelligent Sensing, and Mechatronics (PRISM) Laboratory

3141 Chestnut Street, MEM Department, Room# 2-115

Drexel University, Philadelphia, PA 19104, USA

{teeranoo, desai, alau}@coe.drexel.edu

Abstract

Reality-based modeling of deformable tissues is critical for providing accurate haptic feedback to the surgeon in common surgical tasks such as grasping and cutting organs/tissues. In reality-based modeling, we are interested in modeling tissues as accurately as possible by determining the mechanical properties experimentally and developing a predictive model that is self consistent with the experimentally-determined properties. In this paper, we present the newly developed hardware and software to characterize the mechanical response of pig liver during (ex-vivo) cutting. The macroscopic cutting force-displacement curve shows repeating self-similar units of localized linear loading followed by sudden unloading. The sudden unloading coincides with onset of localized crack growth. This experimental data was used to determine the self-consistent local effective Young's modulus of the specimens to be used in finite element models. Results from plane-stress and plane-strain finite element analyses reveal that the magnitude of the self-consistent local effective Young's modulus varies within close bounds.

Keywords: Reality-based haptic display, Liver cutting, Surgical simulation, Robot-assisted surgery.

1. Introduction

Modeling the response of a deformable soft tissue during cutting is a fundamental requirement for developing a reality-based haptic interface for robot-assisted surgery. Our ongoing research focuses on modeling and interaction with tissues/organs for robot-assisted surgery. In particular, we are interested in hepatic (liver) tumor biopsies and simulating the cutting forces for surgical residents. The liver is composed of lobules held together by an extremely fine areolar structure and covered by a serous and a fibrous coat. While electrocautery and ultrasonic dissection are the most preferred approach for cutting in liver surgery, our surgeon collaborators indicate that there are specific circumstances where the use of a scalpel is necessary. One of those specific circumstances is liver biopsy. Cutting with a scalpel allows better identification of margins without cellular distortion (as is caused in electrocautery). Thus, for liver biopsies (done with a scalpel), it is critical that the surgeon does not cut the area around the tumor too deep and too long by applying excessive force (with each cut) as the serous

and fibrous coat will rapidly tear leading to excessive bleeding and life threatening conditions. For such a procedure, the resident and surgeon should have opportunities to familiarize themselves with the complexities in a liver biopsy before operating on patients. Such familiarization can be accomplished via real-time virtual simulation of the procedure. Success of real-time virtual simulation requires the development of three ingredients: (i) a reality-based tissue model to produce the interaction forces experienced during an actual biopsy, (ii) a model capable of updating the geometry and topological changes due to cutting via dynamically re-forming the mesh as the tissue-cutting process proceeds, and (iii) computationally non-intensive approaches tailored for real-time simulation.

This paper presents results of our ongoing work to develop a reality-based model whereby the effective properties of the tissue are self-consistent with actual experimental data of interaction forces measured during tissue cutting. In the literature, most modeling efforts are focused towards assuming the mechanical properties and developing methods to efficiently solve the tissue simulation problem for robot-assisted surgery/training. Current approaches to modeling deformation of organs are either geometry-based or physics-based. In the geometry-based methods [1, 2], the deformations are purely based on geometric manipulations without taking into account the dynamic interactions within the object. Physics-based models simulate the physical behavior of objects and take into account the internal and external forces. Physics-based models are computationally intensive and utilize particle-based schemes [3], finite element methods [4-6], or meshless methods [7]. However, most of these methods assume a linear elastic model and hence the computations are done offline before the actual simulation begins. Since soft tissue is highly inhomogeneous and nonlinear [8], direct application of finite element modeling with refined mesh incorporating non-linearity is computationally intensive for real time simulation. Basdogan proposed a real time simulation of dynamically deformable finite elements models using modal analysis and spectral Lanczos decomposition [9]. This method minimizes the complexity of the computation in real time at the expense of realism of the model.

Modeling tissue cutting has been explored to a limited extent and till date there does not exist a standard methodology for realistic simulation of the cutting process. Most of the work in literature does not take into account the physics behind cutting (such as energy exchange). Resolved-force haptic devices such

¹ We would like to acknowledge the support of National Science Foundation grants EIA-0079830 and CAREER award IIS-0133471 for this work.

² Corresponding author.

as the Phantom from SensAble Technologies have been used to display external cutting forces of a single blade in surgical procedures, however, they are not reality-based [10, 11]. There exists a limited body of literature focused on the effect of cutting biological tissues on global deformations. Scissors cutting data was gathered for biological tissues by Greenish and Hayward, but not modeled [12]. Many researches describe modeling of cutting linear elastic objects as cutting meshes in the finite element model. Cotin et al [13] proposed cutting as a change in topology. A hybrid method called “tensor spring” related to particle-based method has also been introduced. It uses elastic modeling with pre-computations yielding a tensor mass model with real time ability. However, in reality, cutting simulation based on conventional FEM model frequently breaks down due to difficulties from localized tissue fracture and contact mechanics involved in the process [14].

The work presented in this paper has three primary goals. Firstly, we are interested in designing and developing a liver tissue cutting equipment capable of accurately recording the cutting forces and the cut-length in real-time. Secondly, we are interested in conducting experiments to measure the cutting force versus cut-length during liver cutting. Finally, we are interested in determining the local effective Young’s modulus of the tissue that is self-consistent with characteristics of the actual cutting force measured during cutting. The results from these studies will enable us to develop a haptic display capable of representing the cutting forces in liver cutting.

2. Method

This section is divided into three parts: a) design and development of the liver tissue cutting equipment, b) experimental procedure for measuring the liver cutting forces, and c) determination of self-consistent local effective Young’s modulus of the liver tissue.

2.1 Design and development of the liver tissue cutting equipment

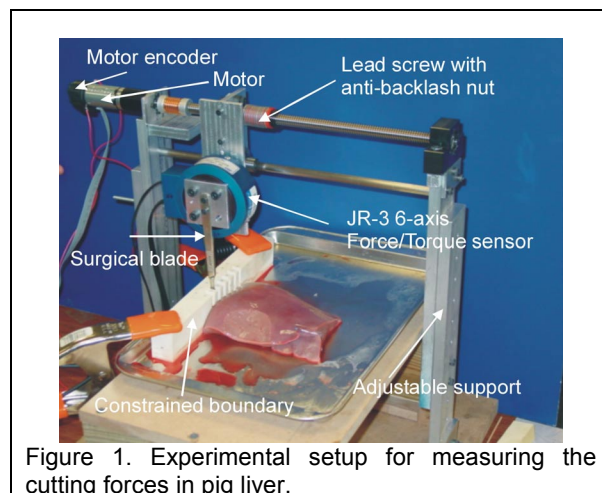


Figure 1. Experimental setup for measuring the cutting forces in pig liver.

The equipment consists of a scalpel-blade cutting subsystem, a computer control subsystem, a digital data-acquisition subsystem, and a data post-processing subsystem (see Figure 1). The test equipment to measure the liver cutting forces was designed to have multiple capabilities such as: a) varying the angle of cutting the liver, b) height adjustment of the scalpel by moving the cutting mechanism over a vertical column to control the depth of cut, and c) variable cutting speed (to measure the effect of cutting speed on cutting forces and strain rates within the specimen). In this paper, we have only analyzed the data for the cutting force vs. the displacement from the constrained boundary. The constrained boundary shown in the figure was designed to simulate the attachment of the liver on one end as in a human body (such as the attachment to the diaphragm).

The cutting mechanism consists of two vertical supports that can be adjusted in the range of 1 to 2 feet from the base, a lead screw assembly with a geared DC motor and an incremental encoder (manufactured by Maxon Motors), and a JR3 precision 6 axis force/torque sensor (model 85M35A-I40) to which a surgeon’s scalpel is attached. We used the number 10 Bard-Parker stainless steel surgical blade in our experimental studies. The cutting blade traverses linearly based on the rotary motion of the DC motor. An anti-backlash nut connects the lead screw to the force sensor. The scalpel is screwed to the force sensor and the force sensor is mounted on an aluminum plate with one end attached to the anti-backlash nut traveling along the lead screw and the other end on a lower guiding shaft (parallel to the lead screw) with a linear bearing to provide low friction linear travel. The assembly has been designed to provide 8 inches of travel distance for cutting the liver specimen. The dSPACE DS1103 controller board (manufactured by dSPACE, Inc.) records the position and force data from the motor’s encoder and force sensor in real-time. We have implemented a proportional + derivative (PD) controller to enable precise movement of the motor (and hence the cutting blade during cutting tasks).

2.2 Experimental procedure for measuring liver cutting forces

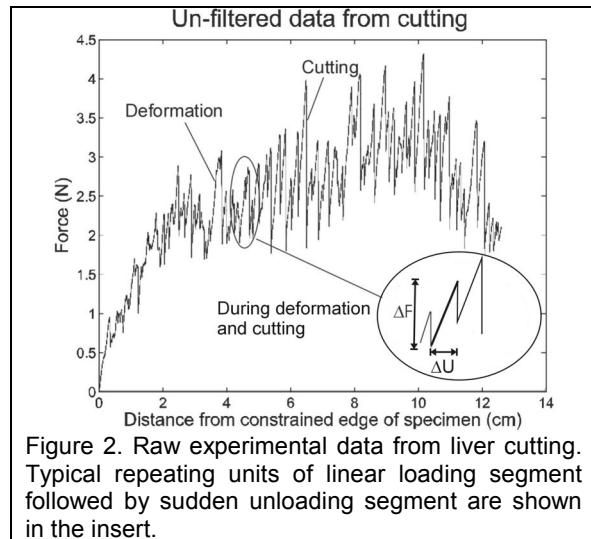
The liver was obtained from freshly slaughtered pigs and transported to the laboratory within 2 hours post mortem. During the experimental setup, the liver was placed on a bed of saline soaked gauze, sprayed with saline and sealed in a container. The saline solution was prepared at room temperature. The tissue sample was not preconditioned because in livery biopsy the cutting forces experienced by the surgeon are on non-preconditioned tissues.

Before starting the experiment, the pig liver was cut into specimens of size 8x12x2.5 cms. The outer encapsulated surface was not cut since we were interested in measuring the cutting forces on the liver. The outer rim of the specimen was covered with

petroleum jelly to minimize moisture loss during the experiment. A bar of rectangular shape made of machineable plastic with an array of small nails clamped at the bottom end penetrated through one edge of the liver specimen to simulate a single constrained boundary surface. While this is not an exact replication of the boundary conditions for a human liver (which is partially attached one end to the diaphragm) this is a none-the-less a valid simplification for our initial tests and model (based on our discussions with the surgeon collaborators).

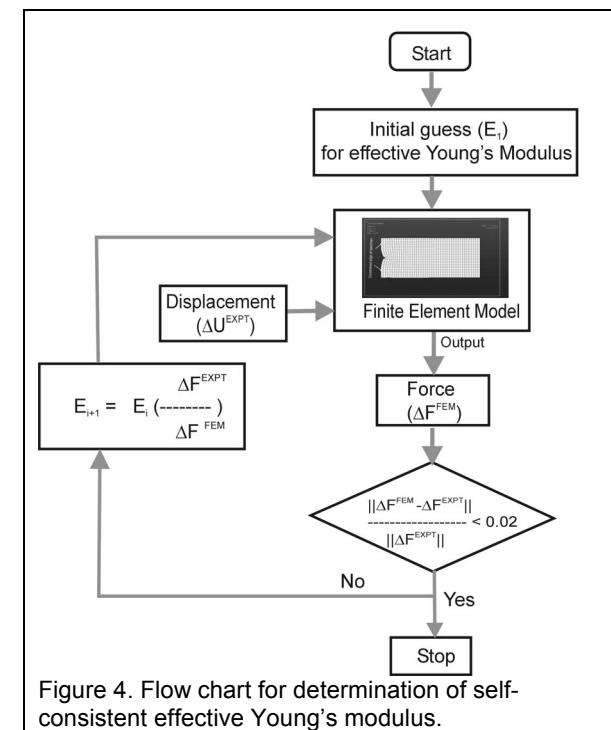
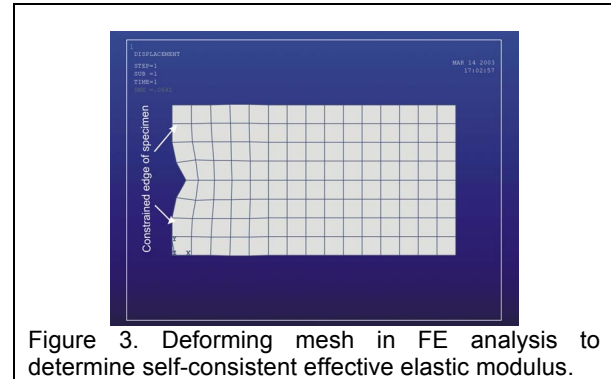
2.3 Determination of self-consistent local effective elastic modulus for finite element analysis

It is desirable to construct a predictive computational model that can simulate the cutting process and predict the mechanical response (cutting force versus cutting-blade displacement characteristics) during liver cutting. To be of real-time application, this simulation model should not be computationally intensive. We propose to use two-dimensional finite element (FE) models for this purpose. A plane-stress FE model is most appropriate for simulating the cutting of very thin liver specimens in which the through-thickness stress is negligible. To cover the range of liver thickness encountered in actual cutting, we also propose to conduct simulation with plane-strain FE models. A plane-strain FE model is most appropriate for very thick liver specimens in which the through-thickness strain is negligible. Simulation results from both plane-stress model and a plane-strain model will bracket the actual mechanical response of liver specimens of various thicknesses.



We observed from experimental data that during liver cutting (quasi-static analysis; scalpel moved at 0.1cm/sec), the cutting force versus cut-length data showed many repeating segments of localized monotonic loading deformation followed by sudden unloading. During each of the localized loading deformation segment, the cutting force increased

linearly with the displacement of the cutting blade (Figures 2 insert). A good simulation model should be able to predict this localized linear loading response consistent with the experimental observations. We propose that in future computational simulations of cutting, two-dimensional FE models with as coarse mesh as possible be used to attain computational efficiency. To obtain high fidelity in the simulated interaction forces, we propose to assign the finite elements with local “effective elastic modulus” that is self-consistent with experimentally measured tissue-cutting force-displacement data.



To determine the self-consistent effective Young's Modulus, we conducted elastic FE analysis for each of the linear monotonic loading segments in the experimentally measured force-displacement curve (Figure 2 insert). A typical FE model of the liver specimen was constructed with 4-noded quadrilateral elements (Figure 3) using the ANSYS general-purpose

finite element software (Release 5.7.1). The procedure to systematically determine the local effective elastic modulus is summarized in Figure 4. To start the procedure, Poisson's ratio of 0.3 and an initial estimated Young's modulus of arbitrary magnitude E_1 was assigned to the elements. Then: a) we applied the experimentally measured ΔU^{EXPT} (see insert of Figure 2) of the loading segment to the FE node that models the cutting blade, b) performed the FE analysis, and c) compared the FE-computed force ΔF^{FEM} of that node to the experimentally measured ΔF^{EXPT} . In the first iteration, ΔF^{FEM} will generally not be equal to ΔF^{EXPT} , and we systematically updated the new value of the estimated Young's modulus as per Eq. (1) and repeated the process, until the ΔF^{FEM} of the new iteration agreed with the experimentally measured ΔF^{EXPT} .

$$E_{i+1} = E_i \left(\frac{\Delta F^{EXPT}}{\Delta F^{FEM}} \right) \quad \text{for } i = 1, 2, \dots \quad (1)$$

The iteration convergence criterion was:

$$\frac{\|\Delta F^{FEM} - \Delta F^{EXPT}\|}{\Delta F^{EXPT}} \leq 0.02 \quad (2)$$

The final E value so determined was the effective Young's modulus, $E^{effective}$. We determined the effective Young's modulus, $E^{effective}$ using both plane-stress and plane-strain FE analysis. Such an FE model embedded with self-consistent effective elastic modulus would be able to predict the cutting-force characteristic in each of the monotonic loading segments consistent with experimentally-measured values (although the initial model would only be two dimensional).

3. Results

We conducted several experiments to confirm the capability of our liver tissue cutting equipment. Experiments were performed at a preset cutting velocity of 0.1cm/second for a blade travel distance of 12cm. Each liver sample (size of 8x12x2.5 cms) could accommodate four parallel cutting lines. We monitored the actual velocity profile of the surgical blade during the cutting of the liver tissue. The actual velocity profile for each trial of cutting showed constant velocity, consistent with that of the preset velocity. This verified that: a) the controller worked satisfactorily, b) the stiffness of the cutting machine was significantly larger than the stiffness of the liver sample, and c) the motor drive was sufficiently powerful.

Figure 5 shows the plot of preset and actual velocity of the cutting blade. From the figure it is clear that the preset and actual cutting velocity coincide, indicating that the cutting force measurement apparatus was sufficiently stiff. Consequently, we can safely assume that the cutting forces obtained during the experiment are indeed those arising from the interaction forces of the blade with the liver specimen

and that the recorded cutting forces are not reduced by the compliance of the structure on which the cutting equipment is positioned.

During the cutting process, we measured the cutting force vs. distance from the constrained boundary of liver specimen. The cutting blade was programmed to move at constant velocity of 0.10 cm/second with a travel distance of 12 cm. We used the JR3 force sensor to measure the X, Y, and Z components of the cutting force and the norm of these forces was plotted versus the displacement of the cutting blade (Figure 2). Results presented here are from 12 liver cutting experiments. We used 3 liver samples and each sample was cut into 4 stripes spaced approximately 2cm apart.

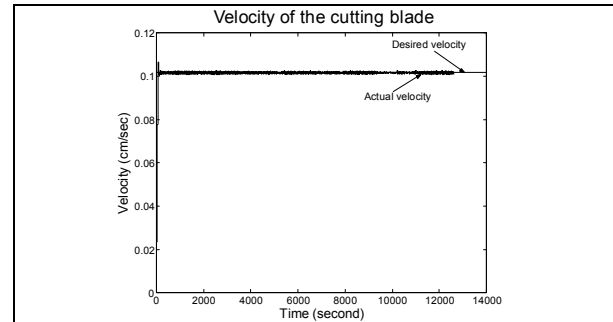


Figure 5. Plot of the preset and actual velocity of the cutting blade during the liver cutting experiment.

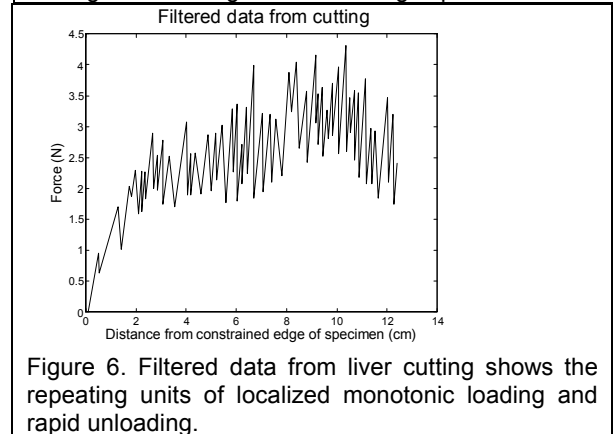


Figure 6. Filtered data from liver cutting shows the repeating units of localized monotonic loading and rapid unloading.

The experimental data revealed that the cutting path was formed by a sequence of repeating units each consisting of a monotonic linear loading segment followed by a rapid unloading segment. Each repeating unit portrayed localized monotonic deformation of the tissue followed immediately by sudden onset of growth of the cut (crack growth). Each visually observed localized blade cut on the tissue clearly corresponded to a sudden drop of the force measured by the force sensor. A filtering procedure was developed to post-process the data to produce a force versus cut-length curve clearly illustrating the "hilltops" and "valleys" of the sequence of localized loading and unloading in the tissue specimen during cutting (Figure 6).

As seen from Figure 6, there is a rise in the cutting force as the cut-length (distance from the constrained

boundary) increases. In Figure 7, we show a sample local monotonic loading segments that we used in estimating the local effective Young's modulus for the specimen. All the liver samples have a characteristic bulge, which leads to more liver tissue being encountered by the blade as the cutting progressed (see liver sample in Figure 1). It is important to note that the liver specimens were not cut into exact right parallelepipeds because we wanted to preserve the capsule of the liver during the cutting process. Our hypothesis is that magnitude of the cutting force directly correlates to the depth of cut. However, we have yet to prove this claim through construction of a testing system, which can monitor the depth of the blade in the liver specimen during the cutting process.

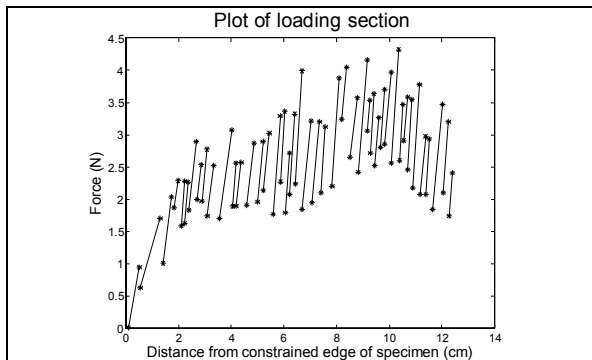


Figure 7. Loading segments during tissue cutting showing linear monotonic deformation.

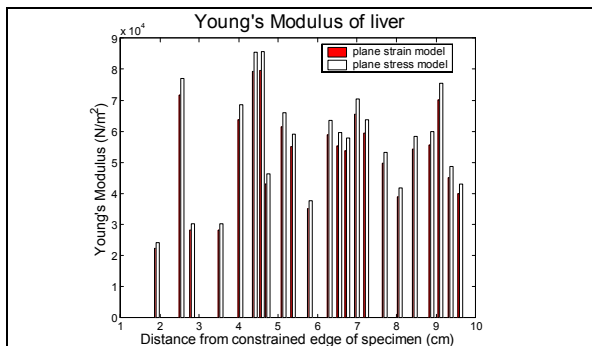


Figure 8. Local effective Young's modulus for the loading segments for a typical cut (plane stress and plane strain analysis).

Results for the local effective Young's modulus for a typical liver cutting are shown in Figure 8. It depicts the effective Young's modulus computed from local deformation data measured at different distances from the constrained boundary. Both values determined from plane-stress FE model and plane-strain FE model are presented. Figure 8 shows that at each location, the modulus values derived from plane stress and plane strain models are very close to each other. Thus, it is reasonable to expect that if a more complicated three-dimensional FE model featuring the exact thickness of the liver is used, the computed effective

Young's modulus will be of very similar magnitude as that determined by our two-dimensional FE models.

Results of 12 liver cuttings are summarized in Table 1. These results reveal that the effective Young's modulus varied from location to location in the liver, but the spatial variation was within reasonable bounds. Overall speaking, the average effective Young's modulus was in the neighborhood of 59,000 N/m² for use with plane-stress model, and 55,000 N/m² for use with the plane-strain model. Table 1 shows that for a given liver specimen, the standard deviation of the average effective Young's modulus (i.e. average of the effective Young's modulus of a typical data represented in Figure 8 over the cut length of the specimen) ranged between 14,000 N/m² and 34,000 N/m². This is expected since the liver tissue is highly non-homogeneous.

Test #	Plane stress model		Plane strain model	
	Young's Modulus x10 ³ N/m ²	Standard deviation x10 ³ N/m ²	Young's Modulus x10 ³ N/m ²	Standard deviation x10 ³ N/m ²
1	59	24	55	23
2	48	15	44	14
3	64	24	60	23
4	72	23	67	21
5	62	23	57	22
6	52	16	49	15
7	100	34	94	33
8	57	21	53	19
9	65	23	60	21
10	56	20	52	19
11	40	19	37	16
12	37	21	34	19
Average	59	16	55	15

Table1. Average effective Young's modulus for each cut on the liver and the corresponding standard deviation.

4. Conclusions and Future Work

A modular liver tissue cutting apparatus has been developed to perform scalpel cutting of liver tissue. It

accurately recorded the liver tissue cutting forces and the motion of the cutting blade. Verification experiments confirm that all subsystems are functioning satisfactorily and that the integrated cutting system is significantly stiffer than the tissue specimen. The equipment is capable of measuring with high fidelity the intrinsic cutting forces versus the cut-length of the tissue specimen. Results from experiments reveal that the cutting process consists of a sequence of intermittent localized extension of the cut in the tissue (crack growth). The measured force-displacement curve shows repeating self-similar units of localized linear loading followed by sudden unloading at the onset of localized fracture. The linear monotonic loading segment of each of these repeating units were used as a vehicle to determine the self-consistent local effective Young's modulus needed for future real-time simulation. The values of the effective Young's modulus determined from plane-stress and plane-strain analyses were very close to each other. Thus it is reasonable to expect that in a three-dimensional FE model utilizing the exact thickness of the liver, the computed effective Young's modulus will be of very similar magnitude.

One observation we have made in our experiments is that the depth of cut has a significant effect on the cutting forces. As a result, our ongoing work is focusing on developing an apparatus, which can measure the depth of the blade in the tissue, thereby allowing us to normalize the cutting forces with the depth of cut. We are also interested in studying the effect of the cutting velocity on the cutting forces. This can be accomplished by using a motor that can accommodate a range of speeds. Finally, from the past literature in tissue biomechanics, many living tissues are nonlinear and inhomogeneous. Hence, our future work will also focus on developing a nonlinear model, which can reproduce the observed cutting forces and localized deformations. The work presented in this paper represents the first step in a series of steps to develop a reality-based haptic interface for modeling the blade-tissue interaction during cutting tasks.

References

- [1] M. A. Srinivasan, "Surface deflection of primate fingertip under line load," *Journal of Biomechanics*, vol. 22, pp. 343-349, 1989.
- [2] J. Edwards and G. Luecke, "Physically based models for use in a force feedback virtual environment," presented at Proceedings of Japan/USA Symposium on Flexible Automation, 1996.
- [3] S. A. Cover, N. F. Ezquerra, J. O'Brien, R. Rowe, T. Gadacz, and O. Palm, "Interactively deformable models for surgery simulation," *IEEE Computer Graphics and Applications*, vol. 13, pp. 65-78, 1993.
- [4] K. Bathe, *Finite Element Procedures*: Prentice Hall, 1996.
- [5] S. Cotin, H. Delingette, and N. Ayache, "Real-Time elastic deformations of soft tissue for surgery simulation," *IEEE Transactions On Visualization and Computer Graphics*, vol. 5, pp. 62-73, 1999.
- [6] D. James and D. Pai, "ARTDEFO: Accurate real time deformable objects," presented at Proceedings of the Computer Graphics (SIGGRAPH), 1999.
- [7] S. De, J. Kim, and M. A. Srinivasan, "A meshless numerical technique for physically based real-time medical simulations," presented at Proceedings of the Medicine meets virtual reality, 2001.
- [8] Y. C. B. Fung, "Elasticity of soft tissues in simple elongation," *American Journal of Physiology*, vol. 213, pp. 1532-1544, 1967.
- [9] C. Basdogan, "Real-Time Simulation of Dynamically Deformable Finite Element Models Using Model Analysis and Spectral Lanczos Decomposition Methods," *Proceeding of the Medicine Meets Virtual Reality (MMVR'2001) Conference, Irvine, CA, 2001*.
- [10] D. Bielser and M. H. Gross, "Interactive simulation of surgical cuts.," presented at Proc. Eighth Pacific Conf. on Computer Graphics and Applications, 2000, 2000.
- [11] K. Hirota, A. Tanaka, and T. Kaneko, "Representation of force in cutting operation," presented at Proceedings of IEEE Virtual Reality, 1999.
- [12] S. Greenish, V. Hayward, T. Steffen, V. Chial, and A. M. Okamura, "Measurement, Analysis and Display of Haptic Signals During Surgical Cutting," *Presence*, vol. 11, pp. 626-651, 2002.
- [13] S. Cotin, H. Delingette, and N. Ayache, "A Hybrid Elastic Model allowing Real Time Cutting, Deformations and Force-Feedback for Surgery Training and Simulation," *Virtual Computer journal*, vol. 16, pp. 437-452, 2000.
- [14] M. Mahvash and V. Hayward, "Haptic Rendering of Cutting: A Fracture Mechanics Approach," *Haptics-e, The Electronic Journal of Haptics Research (www.haptics-e.org)*, vol. 2, 2001.